Investigation of rheological behaviors of aqueous gum Arabic in the presence of crystalline nanocellulose

Jones, K.L., Hu, B., Li, W., Fang, Y., Yang, J.

Carbohydrate Polymers Technologies and Applications xxx (xxxx) 100243

Contents lists available at ScienceDirect

Carbohydrate Polymers Technologies and Applications

journal homepage: www.elsevier.com

Investigation of rheological behaviors of aqueous gum Arabic in the presence of crystalline nanocellulose

Kevin L. Jones [a], Bing Hu [b], Wei Li [a], Yapeng Fang [c], Jixin Yang [a, *]

[a] Faculty of Arts, Science and Technology, Wrexham Glyndwr University, Plas Coch, Wrexham, LL11 2AW, United Kingdom
[b] Key Lab of Biotechnology and Bioresources Utilization of Ministry of Education, College of Life Science, Dalian Minzu University, Dalian 116600, China
[c] Department of Food Science and Technology, School of Agriculture and Biology, Shanghai Jiao Tong University, Shanghai 200240, China

ARTICLE INFO

Keywords:
Crystalline nanocellulose
Gum Arabic
Viscosity
Rheological behavior

ABSTRACT

An investigation on the effects of addition of crystalline nanocellulose (CNC) on both the intrinsic viscosity and rheological behavior of gum Arabic (GA) is undertaken. An adapted, facile method of CNC synthesis from microcrystalline cellulose (MCC) is used. At low concentrations of both CNC and GA, intrinsic viscosity of GA appears unaffected. However, the rheological behavior of 20 wt% and 40 wt% GA solutions is markedly affected by the introduction of CNC, even at very low concentrations. Enhanced viscosity and shear thinning properties are demonstrated with increased addition of CNC within the range studied, as are similar increases in storage modulus. Mechanisms are proposed for interactions between GA and CNC that may cause the observed effects, based on previous studies found in the literature. The use of CNC as a food grade viscosity modifier of GA and likely other polymer solutions is confirmed, and suggestions for further investigation are provided.

1. Introduction

Rheological properties of hydrocolloid suspensions continue to attract the attention of researchers and commercial interests across a broad range of fields (De, Malpani, Das, Mitra & Samanta, 2020; Farahmandfar & Naji-Tabasi, 2020; Liu, Shim, Tse, Wang & Reaney, 2018; Wei, Guo, Li, Ma & Zhang, 2021). Tailored rheology of such formulations plays a crucial role in optimizing both industrial processes and the characteristics of a final product.

Gum Arabic (GA) is a natural biopolymer produced from the sap exuded by the Acacia tree. It is 'generally recognized as safe' (GRAS) by (Vikulina, Voronin, Fakhrullin, Vinokurov, & Volodkin, 2020) and is widely used in the pharmaceutical, cosmetic and food industries as a binder, stabilizer, emulsifier/encapsulating material and occasionally as a thickening agent. GA is a complex polysaccharide with a highly branched structure, consisting chiefly of galactose, arabinose, rhamnose and glucuronic acid. There are abundant hydroxyl and carboxyl groups throughout the structure, with the latter carrying negative charges above solution pH of 2.2 following deprotonation of the glucuronic acid constituent (Gashua, Williams & Baldwin, 2016; Sabet et al., 2021). GA solutions display an unusually low viscosity when compared to other polysaccharides of a similar molecular weight, and at high shear rates (10 s^{-1} and above) Newtonian behavior is observed, even at concentrations up to 30 wt% (Sanchez, Renard, Robert, Schmitt & Lefebvre, 2002). In order to extend the utility of GA, there is a need to bestow a controllable viscoelastic behavior to its solutions. Such modifications may allow GA to perform several functions within formulations, furthering the scope for its potential applications.

Crystalline nanocellulose (CNC), sometimes referred to as cellulose nanocrystals or nanocrystalline cellulose, is extracted from natural cellulose fibers which can be found in abundance in nature. Wood, cotton, hemp and plant species in general make up the most common sources, which also lend themselves to the valorization of waste streams of such materials, including biomass and civic refuse. It can also be naturally produced by certain algae, bacteria and tunicate. This combination of sustainability, renewability and natural abundance makes CNC an attractive material. In addition, it is inherently highly biocompatible, and the parent material boasts GRAS status, making it of increasing interest to researchers, particularly in those industries mentioned above.

Extraction of CNC from plant-based materials usually involves a strong mineral acid used at elevated temperature to remove lignin, non-crystalline regions and other impurities which are more susceptible to attack from the acid than highly crystalline regions (Dong, Revol & Gray, 1998; Hamad & Hu, 2010; Revol, Bradford, Giasson, Marchessault & Gray, 1992). The resulting mixture requires several washes in a centrifuge followed by dialysis against DI water to bring the

* Corresponding author.
E-mail address: j.yang@glyndwr.ac.uk (J. Yang).

https://doi.org/10.1016/j.carpta.2022.100243
2666-8939/

pH to around 6–7 and produce the final suspension (Araki, Wada, Kuga & Okano, 1998). Sulfuric acid is commonly employed in the hydrolysis, as residual negative sulfate ions on the exterior of the CNC provide electrostatic repulsion against aggregation of particles, consequently stabilizing the whole system (Dong et al., 1998). Even so, a period of ultrasound treatment is required to fully disperse the nanocrystals. The product can be lyophilized and redispersed with further sonification if required (Hamad, 2017).

In isolation, dispersions of CNC have been well studied and shown to exhibit chiral nematic ordered structures that contribute to the endowment of potentially useful hydrocolloidal properties, although these are strongly dependent on cellulosic source, particle size, aspect ratio and charge (Bercea & Navard, 2000; Lima & Borsali, 2004; Orts, Godbout, Marchessault & Revol, 1998; Revol et al., 1994). The degree of sonication used to disperse CNC in suspension has also been investigated. Although Beck, Bouchard and Berry (2011) found that particle size and surface charge were unaltered by application of high levels of ultrasound, it was suggested that the pitch of chiral nematic phases is affected, resulting in a variation in rheological properties, the latter being confirmed by Shafiei-Sebet, Hamad and Hatzikiriakos (2012). Effectively, a higher level of sonication resulted in a lower viscosity, attributed to both the breaking up of CNC aggregates and ordered domains within the suspension. However, it is consistently evident in the literature that CNC displays high viscosity and remarkable shear thinning properties (Hubbe et al., 2017; Moberg *et al.*, 2017; Chen, Xu, Huang, Wu & Lv, 2017). This suggests that CNC would be a useful additive to modify the rheological properties of liquid materials. Surprisingly, the literature offers very little in the way of studies in this area.

Composites using CNC have been widely investigated at an increasing rate within the food industry, as reviewed by Ahankari, Subhedar, Bhadauria and Dufresne (2021). Kang, Xiao, Guo, Huang and Xu (2021) demonstrated the efficacy of a GA/CNC food grade packaging matrix with the ability to form strong, thermally stable films and protect against oxidation and water vapor. Similar studies can also be found in the literature (Jafari, Bahrami, Dehnad & Shahidi, 2018; Vigneshwaran, Ammayappan & Huang, 2011). This suggests that food grade applications of GA/CNC systems are worth pursuing, *e.g.* in terms of their safety (Huang, Liu, Chang & Wang, 2020).

1.1. Objective

The aim of this work is to study the effects of low concentrations of CNC on the behavior of GA solutions. CNC is extracted from MCC for ease of synthesis and homogeneity of product. An adapted method of synthesis is provided that is facile and well documented, for the benefit of fellow researchers. An investigation into intrinsic viscosity in the dilute regime is undertaken in addition to the rheological effects of varying amounts of CNC solutions within 20 wt% and 40 wt% GA samples to gain new insight into possible synergistic effects between CNC and GA (as a model nanocomposite). It is hypothesized that CNC can be shown as an effective viscosity modifier, with a view to informing further work on food grade formulations for future applications.

2. Experimental

2.1. Materials

Microcrystalline cellulose (MCC) (Avicel PH-101, Sigma Aldrich) and 1.83 specific density sulfuric acid (Fisher Scientific) were used as received. GA was provided by Starlight Product (France) with stated molecular weight (Mw) 552 kDa and polydispersity index of 2.54. Deionized water was taken from a Purite Select purification system and showed resistivity of 18.2 MΩ.

2.2. CNC synthesis

The method used is adapted from the general acid hydrolysis process described by Hamad (2017) where wood pulp is used as starting material. It was developed as a facile process, providing a consistent, reproducible product. A 1:8 wt ratio of MCC and 64 wt% sulfuric acid was used in the synthesis. MCC was mixed with DI water in an ice bath under magnetic stirring, forming a slurry. Whilst maintaining the slurry in the ice bath and ensuring temperature remained below 50 °C, stock sulfuric acid was added dropwise until the mixture contained MCC and a 64 wt% acid solution in the required (1:8) weight ratio, this process taking approximately 5 min. The mixture was immediately transferred to a water bath at 45 °C and stirred vigorously at this temperature for 30 min. It was then quenched in DI water equivalent to 10 times the total mixture weight at room temperature with stirring for 10 min to stop the hydrolysis process.

After being left overnight, the mixture separated into an ivory-white, turbid bottom layer making up approximately 1/5 of the total volume, and a clear upper layer, of which approximately 3/4 was removed. At ambient temperature, the remaining mixture was stirred for a further 10 min before washing four times for 5 min at 5300 rpm in a Labofuge 200 centrifuge (Heraeus). For each wash, the clear supernatant was removed and replaced with fresh DI water which was shaken with the remaining sediment. If the mixture remained turbid (not separated) after any centrifuge cycle, then the process was considered complete.

The washed mixture was stirred for 5 min before commencing dialysis against DI water in a 14.6 kDa membrane where the water was replaced daily until a constant pH of approximately 6 was attained for over 24 h, usually requiring a total of 5 days. At this point the suspension was sonicated in a SONIFER 450 (Branson) at power level 7 with intermittent cycle in an ice water bath for a total of 30 min to disperse any CNC aggregates. It was then frozen thoroughly before freeze-drying. Reconstituted, smaller volumes of aqueous suspensions used were sonicated in an ice bath for 20 min using Soniprep 150 (MSE) at amplitude of 22 μm.

2.3. Characterizations of CNC

2.3.1. Scanning electron microscope (SEM)

A Hitachi S-4800 field emission scanning electron microscope (FE-SEM) was used to capture the micrographs at an accelerating voltage of 4 kV. All samples were fixed on top of a conductive tape mounted on a sample stub and coated with a thin gold layer before SEM imaging.

2.3.2. Transmission electron microscopy (TEM)

High resolution TEM images were taken using JEOL JEM-2100F field emission electron microscope at operating voltage of 200 kV. The specimens used for TEM studies were dispersed in absolute ethanol by ultrasonic treatment. The sample was then dropped onto a copper grid coated with a holey carbon film and dried in air.

2.3.3. X-ray diffraction (XRD)

X-ray diffraction (XRD) analysis was carried out using a Shimadzu XRD-6000 X-ray diffractometer (Shimadzu Corporation) equipped with a monochromatized Cu-Ka source. The scanning range of 2θ was between 2.0 and 80.0, with a scan speed of 2.0°/min. Shimadzu profile-fitting analysis was used to generate integrated intensity of the selected peaks (Shimadzu XRD-6000 software version 4.1). The relative crystallinity was calculated by the ratio of each characteristic peak area to the total area of a diffractogram (which is the sum of peak areas and amorphous areas) expressed as a percentage.

2.3.4. Zeta potential (ζ)

Zeta potential was determined by particle electrophoresis using a Nano-ZS Zetasizer (Malvern). Low sample concentrations of approximately 0.05 wt% were used to minimize multiple scattering effects and equilibrated at 25 °C during analysis.

2.4. Intrinsic viscosity investigation

A calibrated Ubbelohde viscometer (Cannon Ubbelohde Calib 75) was used to measure flow times of solvent (DI water), GA solution of varying concentrations in isolation, and CNC suspension of varying concentrations in isolation. In each case, 20 ml of most concentrated solution was measured first, and dilution of samples was achieved by removing some liquid and replacing with equal amounts of DI water such that the volume used each time was 20 ml. For the mixture of GA and CNC, the sample was made up of 10 ml GA solution and 10 ml CNC suspension of equal concentrations. In the latter case, the wt% was taken as the sum of GA and CNC. Fresh samples were made up for each concentration of CNC.

The viscometer was suspended in a water bath which was kept at 20 ± 0.1 °C. Three consecutive flow times for each sample were obtained within 1 s. Given the nature of stopwatch measurements, an intraclass correlation coefficient test was performed to evaluate reliability and reproducibility of results. A two-way random effects model, with absolute agreement relationship, and single rater units was used.

2.5. Rheological investigation

Rheological investigation was undertaken using an AR500 rheometer (Texas Instruments). A geometry of 40 mm flat steel plate was used for all tests in 2.5.1 and 2.5.2.

2.5.1. Viscosity

With a plate gap of 400 μm and equilibrated temperature of 25 °C, the viscosity of 20 wt% GA solution and the effects of introducing small amounts of CNC were determined. The average of triplicate steady-state shear viscosity measurements was taken in the range 0.1 to 500 Hz and included both ramping up and immediate ramping down conditions.

For samples involving mixtures of GA and CNC, each measurement consisted of equal amounts of 40 wt% GA solution and CNC suspension, giving final GA concentration of 20 wt%. Each CNC suspension used was sonicated in a Soniprep 150 (MSE) at amplitude of 22 μm for 5 min before analysis in isolation or addition with GA.

2.5.2. Effects of temperature and frequency on storage (G') and loss (G'') moduli

The same geometry was employed as in 2.5.1. In order to accommodate this, a 40%wt GA solution was used such that a useful linear viscoelastic region (LVR) could be studied. LVR was established using a stress sweep between 0.8 and 200.0 Pa and subsequent analyses were performed within this domain. A plate gap of 500 μm and equilibrated temperature of 20 °C was used for each analysis. Each sample was prepared by combining varying amounts of CNC solution (sonicated as in 2.5.1) with GA and made up with DI water resulting in 40 wt% GA and known%wt of CNC. Samples were analyzed to observe the effects of increasing temperature and increasing oscillation frequency on G' and G'' to examine their internal structure and mechanical properties. A temperature ramp from 10 °C to 50 °C and frequency sweep from 0 to 250 rad/s was performed independently for each sample three times, with average values used.

3. Results and discussion

3.1. Characterization of synthesized CNC

Figure S1 (see Supplementary Materials) shows the appearance of CNC mixture, suspension and dried product at various stages in the synthesis process. During the initial hydrolysis, a discoloration of the mixture to light yellow/brown was observed, caused by side reactions such as dehydration and being in accordance with that noted in the literature (Dong et al., 1998). Washing removed the discoloration and the final freeze-dried product presented as a white, diaphanous solid, forming localized, brittle shards, as described by Fahanwi and Yildiz (2018). On handling the final product, smaller particles could be seen moving due to electrostatic forces, indicating that negative charge had been successfully bestowed onto the material.

3.1.1. Morphologic characterization of CNC

SEM analysis was performed on the synthesized material with no further treatment. The images of products are shown in Figure S2 (see Supplementary Materials). Formation of extremely thin film sheets can be seen with occasional protrusions of aggregated CNC crystals (approximately 10 μm and above in length) that appear irregular in size and shape. These also present as randomly orientated.

TEM analysis was performed on the synthesized material with no further treatment and the resulting images are shown in Figure S3 (see Supplementary Materials). TEM analysis offers more information in terms of dimensions and morphology of individual crystals. The smallest individual crystals have needle-like structures of length ranging from 200 to 400 nm, all with characteristic high aspect ratio (Kaushik, Fraschini, Chauve & Moores, 2015). Larger agglomerates can also be seen, highlighting the requirement for sonication in order to release individual crystals in aqueous suspension.

3.1.2. XRD

X-ray diffractogram representation from data points is shown in Figure S4 (see Supplementary Materials). The peaks at 17◦, 23◦ and 34◦ are characteristic of freeze-dried CNC (Hamad, 2017; Park, Baker, Himmel, Parilla & Johnson, 2010) and were used in calculating the crystallinity index (CI). After baseline adjustment, CI was calculated as a percentage ratio of those peaks characteristic of CNC to the total area of the diffractogram using the formula:

$$\%CI = [(Sum\ of\ area\ under\ characteristic\ peak \times s) / (total\ area)] \times 100$$

Using this method, CI was found to be 76.4%.

3.1.3. Zeta potential

Zeta potential was found to be −23.5 mV with a standard deviation of 6.2 mV, confirming an appreciable negative surface charge present on CNC particles.

3.2. Intrinsic viscosity (dilute regime)

Fig. 1 shows plots of 'reduced viscosity' (ηred) in blue, and the natural log of 'relative viscosity' divided by concentration [ln(ηrel)/c] in orange. Measurements were taken for GA in isolation, CNC in isolation, and equal amounts of GA and CNC at various concentrations. The sum weight of GA and CNC was used to determine the concentration in the latter.

The intrinsic viscosity is given by the y-intercept of the lines. Ideal results would have identical y-intercepts for both lines. For CNC in isolation and the GA/CNC mixture, an average of the intercepts gives intrinsic viscosity values of 0.29 and 0.42, respectively. A notable discrepancy between Huggins and Kraemar intercepts exists for GA in isolation, ranging from 0.67 to 0.78. However, all plots throughout have a

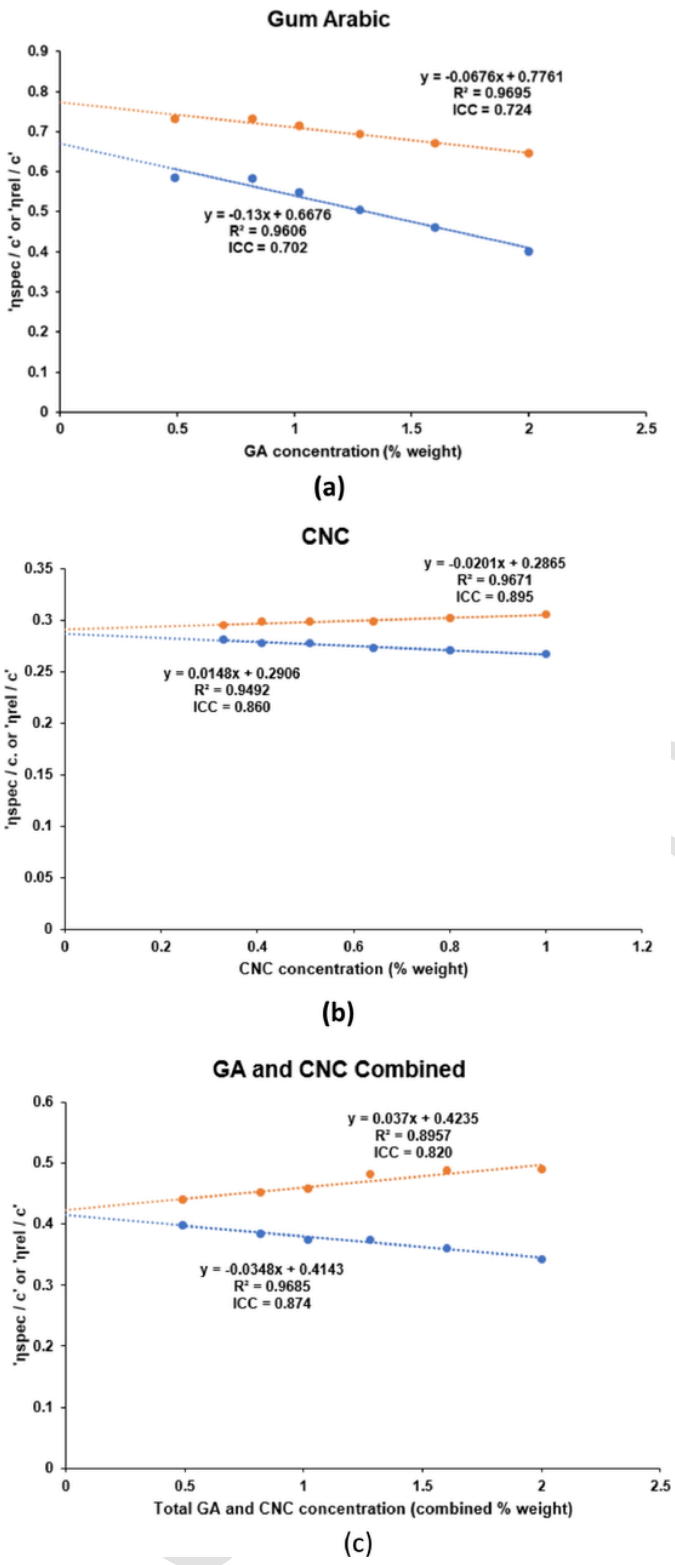

Fig. 1. Huggins (blue) and Kraemar (orange) plots for GA (a), CNC (b), and GA/CNC mixture (c).

high correlation coefficient and ICC analysis shows moderate (GA) to good (CNC and mix) reliability. This shows that not only the mean values have strong correlation, but there are also reliability and reproducibility within each group of measurements used to find that mean, further strengthening the validity of the results. For GA comparison, Mothe and Rao (1999) obtained intrinsic viscosity value close to this range (0.60) using analytical grade GA. Even so, this far exceeds those for CNC and the GA/CNC mixture. Indeed, if one combines the values for the latter two (0.71), we arrive at a figure that lies centrally within the range for GA in isolation. This could suggest that in the dilute regime the contributions towards intrinsic viscosity provided by GA and CNC in the mixture are independent, with GA dominating. The subsequent addition of dilute CNC suspensions merely serves to reduce the intrinsic viscosity by lowering the concentration of GA in solution. Studies have shown that the hydrodynamic radius of aqueous GA remains constant at concentrations below 3 wt% and that overlap occurs over 6 wt% (Li et al., 2009). Physically, the introduction of such small amounts of CNC is unlikely to exclude sufficient volumes to force the colloid into overlapping 'prematurely'. Superficially at least, there is little evidence of any chemical interaction between the materials in this case. A more extensive investigation using a wide range of GA/CNC ratios and concentrations may provide further insight. What does appear evident is that there is no association between GA and CNC in the dilute range studied here that enhances intrinsic viscosity properties.

3.3. Rheology investigation

3.3.1. Viscosity with 20 wt% GA solution

Rheological behaviors of 20 wt% GA solution in isolation and mixtures of 20 wt% GA solution with varying concentrations of CNC are shown in Fig. 2.

Rheological behavior of GA is markedly increased by the addition of CNC suspension. From Fig. 2(a) for example, at low shear rates the viscosity is increased by a factor of 20 with addition of 1 wt% CNC, increasing to a factor of 141 with 4.42 wt% CNC addition. Shear thinning behavior is clearly exhibited at all concentrations within the range studied, in both ramp up and ramp down conditions. At lower CNC concentrations (*i.e.* 1.00 wt% and 1.49 wt%) and shear rates, evidence of a Newtonian plateau can be seen which is not observed for higher concentrations, suggesting that higher concentrations extend the shear thinning regions. This effect also seems evident at higher shear rates where only the lower concentrations appear to be reaching a plateau. In order to confirm that a synergistic effect was observed, the rheological behavior of CNC suspension in isolation was analyzed and Fig. 3 shows the rheology of 2.00 wt% and 4.00 wt% CNC suspensions in isolation, along with selected mixed samples.

This shows the viscosity of mixed samples is not related simply to the summation of individual GA and CNC contributions, and strongly indicates a synergistic relationship between the two materials. There is also clear evidence that increasing concentrations of CNC suspension not only provides a remarkable increase in the viscous behavior of GA solution, but that shear thinning regions are also extended.

One possible explanation for such an extension to shear thinning regions could be provided by considering a previous study by Li et al., 2012 on the arabinogalactan proteins (AGPs) fraction of aqueous GA and its contribution towards viscosity. The study suggested that despite AGP accounting for only 10% of the mass, it may be solely responsible for shear thinning properties *via* interacting micelle formation. Application of shear forces breaks these micelles down into smaller entities which then reassemble through hydrophobic interactions over small timescales in a continuous process.

The presence of CNC in such solutions could increase the rate at which the reforming of micelle networks occurs. The volume excluded by CNC would encourage a higher rate of interaction between loose aggregates. The presence of negative surface charge on CNC particles would then enhance this effect by electrostatic repulsion of charged carboxylic groups both along the polypeptide chain and side groups (Wee, Sims, Goh & Matia-Merino, 2019). This increased rate of micelle reforming would prolong shear thinning effects over a far greater range than GA in isolation, which is observed in the present study.

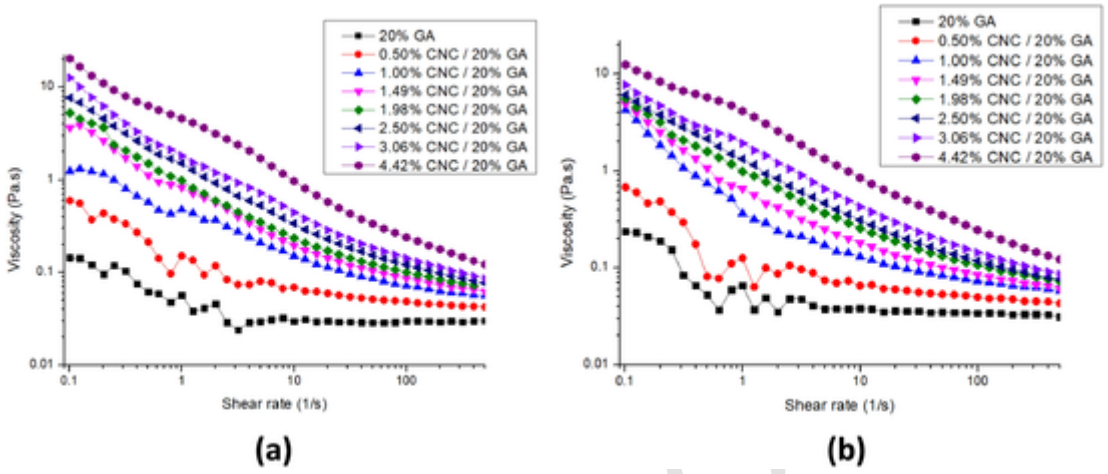

Fig. 2. Steady-state shear viscosity analyses of 20 wt% GA solution in isolation and with varying concentrations of CNC: (a) the ramping up from 0.1 to 500 s^{-1} and (b) the subsequent ramping down from 500 to 0.1 s^{-1}.

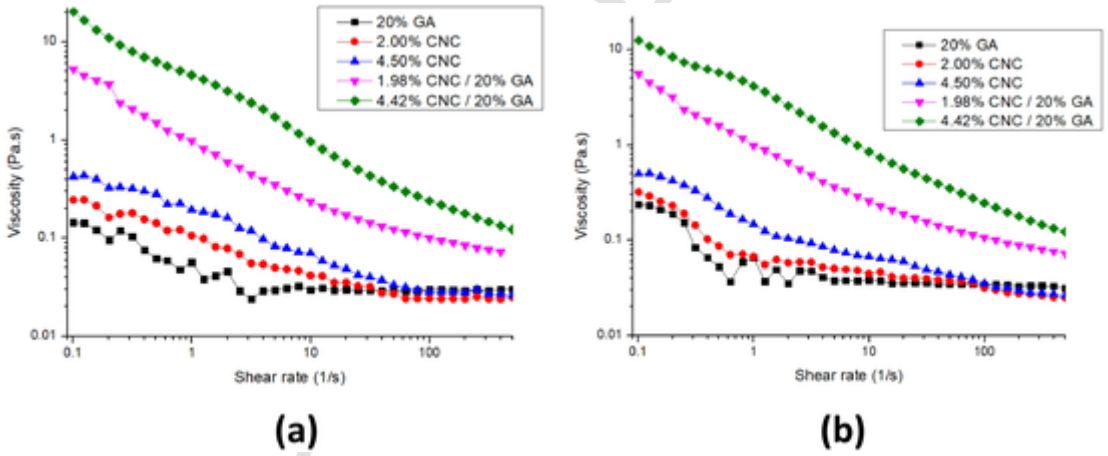

Fig. 3. Rheology of CNC in isolation compared to GA in isolation and selected mixed samples: (a) ramping up from 0.1 to 500 s^{-1} and (b) the subsequent ramping down from 500 to 0.1 s^{-1}.

3.3.2. Effects of temperature and frequency on storage and loss moduli using 40 wt% GA

Strain sweeps of 40 wt% GA in isolation at 10 °C is shown in Figure S5 (see Supplementary Materials). LVR was determined to be between 1 and 2 Pa and these parameters were used in subsequent analyses.

The effects of temperature on storage modulus (G') and loss modulus (G'') of 40%wt GA solutions are shown in Fig. 4. Up to approximately 38 °C (within LVR) there are broad differences in G' between samples, each of which is largely unaffected by temperature. Introduction of small concentrations of CNC imparts a clear increase in the elastic behavior of the solutions. When compared to GA in isolation, addition of 0.5 wt% CNC increases G' by tenfold, with an increase of 300x for 2.0 wt% CNC. This strongly indicates a marked increase in 'solid-like' behavior of the solution when CNC is added. Similarly, addition of CNC is also shown to increase G'', although the effects here are far less severe, with an eightfold increase from GA in isolation to 2.0 wt% CNC addition. Consequently, at concentrations of 2.0 wt% CNC, values for G' and G'' reach relative parity.

Fig. 5 shows that for all samples an increase in oscillatory frequency results in an increase for both G' and G'' at similar rates. Again, a more significant increase in G' is observed than that for G'' between samples. From GA in isolation to 2.0 wt% CNC addition, a 300x increase in G' and tenfold increase in G'' are seen at low frequencies. Once more at 2.0 wt% CNC, G' and G'' have similar values.

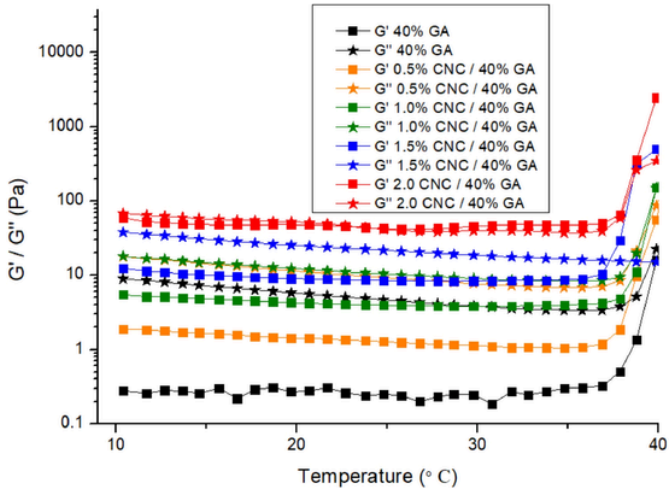

Fig. 4. Temperature ramp from 10 °C to 50 °C for 40 wt% GA solutions with varying CNC concentrations.

Similar rheological effects have been observed and investigated previously (Boluk, Zhao & Incani, 2012; Dickinson & Eriksson, 1991; Kusano et al., 2021), with 2 methods proposed to explain the phenomenon. Firstly, 'polymer bridging' could occur if CNC particles have

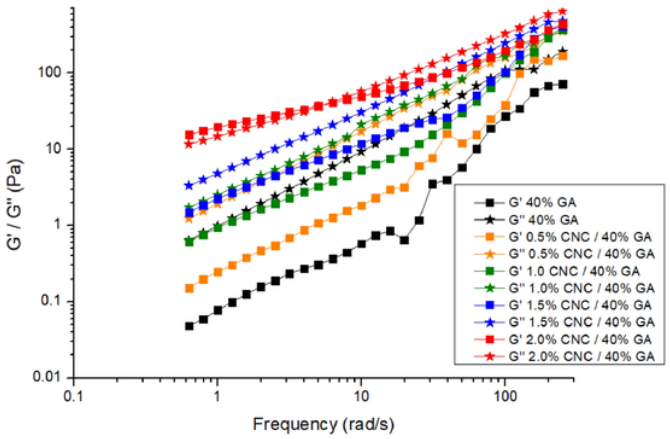

Fig. 5. Frequency sweep of G' and G'' for solutions of 40 wt% GA and varying additions of CNC.

greater affinity for polymer molecules than the aqueous medium and polymer molecules may be adsorbed onto neighboring CNC rods. These molecules may further attach themselves to other rods elsewhere on the polymer chain, resulting in the formation of a network. Secondly, 'depletion flocculation' was proposed if conditions were such that polymer molecules are not adsorbed onto particles. In this case, the volume excluded by GA molecules would lead to more densely packed CNC particles, possibly resulting in agglomeration of CNC particles in suspension. Marchessault, Morehead and Koch (1961) confirmed that an increase in size of CNC particles markedly affects the rheology of CNC suspensions in isolation, although no literature can be found on whether this would confer similar changes in CNC/polymer combinations.

Both mechanisms would explain the lack of synergy in the dilute regime where contact between the two materials is much less likely, thus reducing any bridging or exclusion effects, particularly as both GA and CNC are endowed with negative charge and would experience repulsive electrostatic forces. In the more concentrated regime, where synergy is evidenced, interactions between the two may be inevitable, and one could expect a greater probability of either mechanisms occurring.

Clearly, increases in both G' and G'' will result in increased viscosity as observed. What remains to be seen is the degree to which each modulus is contributing to the overall effects on rheological behavior of the solutions, and which of the proposed mechanisms is more likely to be the cause. One could argue that if the marked increase observed in G' demonstrates that the solutions are becoming increasingly solid-like and that this is the cause, then bridging flocculation is the more likely mechanism as this provides a more (solid-like) structural network. Alternatively, if the (albeit less severe) increase in G'' is found to provide the major contribution to increased viscosity then this may support the argument for depletion flocculation. A key difference between the two is that depletion flocculation assumes that rheology is affected predominantly by CNC agglomeration, whereas bridging requires sustained interaction between the two materials. Further investigation should be aimed at favoring one mechanism over the other. For example, the use of cationically modified CNC may prove very insightful, given that this should greatly encourage bridging between oppositely charged GA and CNC, while lowering depletion effects. This could be further investigated with charge screening electrolytes.

Although care was taken to regiment the sonication of all CNC samples, it should be noted that, as described above, the level of sonication has also been shown to affect the rheology of CNC suspensions in isolation. Although Dong et al. (1998) found that CNC particles in suspension did not further reduce in size after 5 min sonication, they did observe a correlation between increased sonication levels and reduction in viscosity. Shafiei-Sebet et al. (2012) investigated the phenomenon further, showing a difference in viscosity at low shear rates of over two orders of magnitude between non-sonicated and high energy sonicated suspensions. They accounted for the effect by showing that increased sonication decreased the size and structure of chiral nematic domains within the CNC suspension. No subsequent work on this effect being transferred onto CNC/polymer rheology can be found in the literature.

Reducing tests were performed using a range of concentrations for GA, CNC and their mixtures, using Benedict's reagent as per the literature (Mishra, 2019). CNC was found to have no reaction, and GA showed visible reaction at concentrations of 5% and above. Mixtures followed the same behavior of GA in isolation, regardless of CNC content.

What has undoubtedly been evidenced is that while showing little effect in the dilute regime, the addition of small amounts of CNC can be used to impart significant modifications to the viscosity and overall rheology of more concentrated GA solutions.

4. Conclusion

In the dilute regime, inherent viscosity of GA/CNC mixtures appears to be dominated by GA contribution, with no evidence of enhanced viscosity effect by addition of CNC. It is possible that in such conditions, little interaction between the two materials occurs. At higher concentrations (20 and 40 wt% GA), CNC addition at low quantities has been shown to markedly augment rheological behavior of the nanocomposite. Viscosity is greatly increased, shear thinning domain is extended over the ranges studied and marked increases in storage moduli are achieved. CNC suspension is expected to have wide ranging applications for modifying the rheology of polymer solutions, particularly those aspiring to GRAS and food-grade status. Although two mechanisms are proposed to account for this phenomenon ('polymer bridging' and 'depletion flocculation'), further investigation is required for a richer understanding. In addition, gaps in the literature suggest that there is much scope available in terms of optimizing the application of CNC suspensions in the manner used in this study. Parameters such as GA concentration, surface charge, sonication and temperature are proposed as worthy of further investigation. In this work GA is used as a model carbohydrate polymer and should serve to highlight opportunities in developing similar CNC/polymer nanocomposites, particularly those where biocompatibility and sustainable are of high importance.

Uncited references

Vikulina, A., Voronin, D., Fakhrullin, R., Vinokurov, V., & Volodkin, D. (2020). Naturally derived nano- and micro-drug delivery vehicles: halloysite, vaterite and nanocellulose. New Journal of Chemistry, 44, 5638-5655.

Declaration of Competing Interest

The authors declare that they have no known competing financial interests or personal relationships that could have appeared to influence the work reported in this paper.

Acknowledgements

This work was supported by Liaoning Province Livelihood Science and Technology Project (2021JH2/10200019), Department of Education of Liaoning Province (LJKZ0037), Dalian Key Science and Technology Project (2021JB12SN038) in China.

Supplementary materials

Supplementary material associated with this article can be found, in the online version, at doi:10.1016/j.carpta.2022.100243.

References

Ahankari, S., Subhedar, A., Bhadauria, S., & Dufresne, A. (2021). *Nanocellulose in food packaging. A Review. Carbohydrate Polymers*, *255*, 117479.

Araki, J., Wada, M., Kuga, S., & Okano, T. (1998). *Flow properties of microcrystalline cellulose suspension prepared by acid treatment of native cellulose. Colloids and Surfaces A: Physicochemical and Engineering Aspects*, *142*, 75–82.

Beck, S., Bouchard, J., & Berry, R. (2011). *Controlling the reflection wavelength of iridescent solid films of nanocrystalline cellulose. Biomacromolecules*, *12*, 167–172.

Bercea, M., & Navard, P. (2000). *Shear dynamics of aqueous suspensions of cellulose whiskers. Macromolecules*, *33*, 6011–6016.

Boluk, Y., Zhao, L., & Incani, V. (2012). *Dispersions of nanocrystalline cellulose in aqueous polymer solutions: Structure formation of colloidal rods. Langmuir : the ACS journal of surfaces and colloids*, *28*, 6114–6123.

Chen, Y., Xu, C., Huang, J., Wu, D., & Lv, Q. (2017). *Rheological properties of nanocrystalline cellulose suspensions. Carbohydrate Polymers*, *157*, 303–310.

De, A., Malpani, D., Das, B., Mitra, D., & Samanta, A. (2020). *Characterization of an arabinogalactan isolated from gum exudate of Odina wodier Roxb.: Rheology, AFM, Raman and CD spectroscopy. Carbohydrate Polymers*, *250*, 116950.

Dickinson, E., & Eriksson, L. (1991). *Particle flocculation by adsorbing polymers. Advances in Colloid and Interface Science*, *34*, 1–29.

Dong, X., Revol, J., & Gray, D. (1998). *Effect of microcrystallite preparation conditions on the formation of colloid crystals of cellulose. Cellulose (London, England)*, *5*, 19–32.

Fahanwi, A.N., & Yildiz, U. (2018). *Pyrocatechol recovery from aqueous phase by nanocellulose-based platelet-shaped gels: Response surface methodology and artificial neural network design study. Journal of Environmental Engineering*, *145*, 04018140.

Farahmandfar, R., & Naji-Tabasi, S. (2020). *Influence of different salts on rheological and functional properties of basil (Ocimum bacilicum L.) seed gum. International Journal of Biological Macromolecules*, *149*, 101–107.

Gashua, I.B., Williams, P.A., & Baldwin, T.C. (2016). *Molecular characteristics, association and interfacial properties of gum Arabic harvested from both Acacia senegal and Acacia seyal. Food Hydrocolloids*, *61*, 514–522.

Hamad, W.Y. (2017). Hydrolytic extraction of cellulose nanocrystals Ed. In S., Stevens (Ed.), *Cellulose nanocrystals: Properties, production and applications* (1st ed, pp. 33–64). Sussex, England: Wiley.

Hamad, W.Y., & Hu, T.Q. (2010). *Structure–process–yield interrelations in nanocrystalline cellulose extraction. Canadian Journal of Chemical Engineering*, *88*, 392–402.

Huang, S., Liu, X., Chang, C., & Wang, Y. (2020). *Recent developments and prospective food-related applications of cellulose nanocrystals: A review. Cellulose (London, England)*, *27*, 2991–3011.

Hubbe, M., Tayeb, P., Joyce, M., Tyagi, P., Kehoe, M., Dimic-Misic, K., et al. (2017). *Rheology of nanocellulose-rich aqueous suspensions: A review. Bioresources*, *12*, 9556–9661.

Jafari, S., Bahrami, I., Dehnad, D., & Shahidi, S. (2018). *The influence of nanocellulose coating on saffron quality during storage. Carbohydrate Polymers*, *181*, 536–542.

Kang, S., Xiao, Y., Guo, X., Huang, A., & Xu, H. (2021). *Development of gum arabic-based nanocomposite films reinforced with cellulose nanocrystals for strawberry preservation. Food Chemistry*, *350*, 129199.

Kaushik, M., Fraschini, C., Chauve, G., & Moores, J.P.A. (2015). *Transmission electron microscopy for the characterization of cellulose nanocrystals. In K. Maaz (Eds.), The Transmission Electron Microscope - Theory and Applications (pp. 129–164). Rijeka, Croatia: IntechOpen.*

Kusano, T., Kumano, N., Yoshimune, W., Munikata, T., Matsunaga, T., & Harada, M. (2021). *Interplay between interparticle potential and adsorption structure in nanoparticle dispersions with polymer addition as displayed by small-angle scattering. Langmuir : the ACS Journal Of Surfaces and Colloids*, *27*, 7503–7512.

Li, X., Fang, Y., Al-Assaf, S., Phillips, G.O., Nishinari, K., & Zhang, H. (2009). *Rheological study of gum arabic solutions: Interpretation based on molecular self-association. Food Hydrocolloids*, *23*, 2394–2402.

Li, X., Zhang, H., Fang, Y., Al-Assaf, S., Phillips, G.O., & Nishinari, K. (2012). Rheological properties of Gum Arabic solution: The effect of arabinogalactan protein complex. In J.F., Kennedy, G.O., Phillips, & P.A., Williams (Eds.), *Gum arabic* (1st ed, pp. 229–238). Cambridge: Royal Society of Chemistry.

Lima, M.D., & Borsali, R. (2004). *Rodlike cellulose nanocrystals: Structure, properties and applications. Macromolecular Rapid Communications*, *25*, 771–787.

Liu, J., Shim, Y., Tse, T., Wang, Y., & Reaney, M. (2018). *Flaxseed gum a versatile natural hydrocolloid for food and non-food applications. Trends in Food Science and Technology*, *75*, 146–157.

Marchessault, R.H., Morehead, F.F., & Koch, M.J. (1961). *Some hydrodynamic properties of neutral suspensions of cellulose crystallites as related to size and shape. Journal of Colloid Science*, *16*, 327–344.

Mishra, T.K. (2019). *General tests of carbohydrates and their identification. Publishing services* (1st Edition). Gurgaon: Elsevier India Health Sciences.

Mothe, C.G., & Rao, M.A. (1999). *Rheological behavior of aqueous dispersions of cashew gum and gum arabic: Effect of concentration and blending. Food Hydrocolloids*, *13*, 501–506.

Orts, W.J., Godbout, L., Marchessault, R.H., & Revol, J.-F. (1998). *Enhanced ordering of liquid crystalline suspensions of cellulosic microfibrils: A small angle neutron scattering study. Macromolecules*, *31*, 5717–5725.

Park, S., Baker, J.O., Himmel, M.E., Parilla, P.A., & Johnson, D.K. (2010). *Cellulose crystallinity index: Measurement techniques and their impact on interpreting cellulase performance. Biotechnology for Biofuels*, *3*, 10.

Revol, J.-F., Bradford, H., Giasson, J., Marchessault, R.H., & Gray, D.G. (1992). *Helicolloidal self-ordering of cellulose microfibrils in aqueous suspension. International Journal of Biological Macromolecules*, *14*, 170–172.

Revol, J.-F., Godbout, L., Dong, X., Gray, D., Chanzy, H., & Maret, G. (1994). *Molecularly engineered nanocomposites: Layer by layer assembly of cellulose nanocrystals. Biomacromolecules*, *6*, 2914–2918.

Sabet, S., Rashidinejad, A., Melton, L.D., Zujovic, Z., Akbarinejad, A., Nieuwoudt, M., et al. (2021). *The interactions between the two negatively charged polysaccharides: Gum Arabic and alginate. Food Hydrocolloids*, *112*, 106343.

Sanchez, C., Renard, D., Robert, P., Schmitt, C., & Lefebvre, J. (2002). *Structure and rheological properties of acacia gum dispersions. Food Hydrocolloids*, *16*, 257–267.

Shafiei-Sebet, S., Hamad, W.Y., & Hatzikiriakos, S.G. (2012). *Rheology of nanocrystalline cellulose aqueous suspensions. Langmuir : the ACS journal of surfaces and colloids*, *28*, 17124–17133.

Vigneshwaran, N., Ammayappan, L., & Huang, Q. (2011). *Effect of gum arabic on distribution behavior of nanocellulose fillers in starch film. Applied Nanoscience*, *1*, 137–142.

Wee, M.S.M., Sims, I.M., Goh, K.K.T., & Matia-Merino, L. (2019). *Molecular, rheological and physicochemical characterisation of puka gum, an arabinogalactan-protein extracted from the Meryta sinclairii tree. Carbohydrate Polymers*, *220*, 247–255.

Wei, Y., Guo, Y., Li, R., Ma, A., & Zhang, H. (2021). *Rheological characterization of polysaccharide thickeners oriented for dysphagia management: Carboxymethylated curdlan, konjac glucomannan and their mixtures compared to xanthan gum. Food Hydrocolloids*, *110*, 106198.